Taylor & Francis
Taylor & Francis Group

Photonic Quantum Information Applications of Patterned Liquid Crystals

L. MARRUCCI,[1] E. NAGALI,[2] F. SCIARRINO,[2]
L. SANSONI,[2] F. DE MARTINI,[2] B. PICCIRILLO,[1]
E. KARIMI,[1] AND E. SANTAMATO[1]

[1]Dipartimento di Scienze Fisiche, Università di Napoli "Federico II",
Complesso di Monte S. Angelo, Napoli, Italy
[2]Dipartimento di Fisica dell'Università di Roma "La Sapienza",
Roma, Italy

In this paper we review recent results we obtained in the field of photonic quantum information that were made possible by the introduction of patterned non-uniform liquid crystal cells known as "q-plates": (i) the generation of entangled states of polarization and orbital angular momentum of a photon; (ii) the transfer of a qubit of quantum information from the spin to the orbital angular momentum of photons and vice versa; (iii) the Hong-Ou-Mandel coalescence in the same outgoing mode of a beam-splitter of two photons having nonzero orbital angular momentum; (iv) the universal optimal quantum cloning of orbital-angular-momentum-encoded qubits.

Keywords Liquid crystals; orbital angular momentum; quantum cloning; quantum information

Introduction

Although liquid crystals (LC) have found many important applications in photonic devices, very few of them are related to the field of quantum information. Quantum information is an emerging interdisciplinary research area that is based on the manipulation and transmission of quantum states for information and communication technology applications. The elementary unit of quantum information is the so-called "*qubit*", corresponding to a quantum state defined in a two-dimensional Hilbert space, as that arising from two independent basis states. Many past implementations of quantum information processes have been obtained by means of quantum optics, i.e., using the quantum states of photons. A typical choice for encoding qubits in photons is that of using their polarization states (e.g., horizontal H and vertical V, or left-circular L and right-circular R). However, other photonic degrees of freedom are also available to this purpose and a particularly interesting emerging possibility is that of using the so-called *orbital angular momentum* (OAM) of photons

---

Address correspondence to L. Marrucci, Dipartimento di Scienze Fisiche, Università "Federico II", Complesso Universitari di Monte S. Angelo, via Cintia, Napoli 80126, Italy. Tel.: +39-081-676124; Fax: 39-081-676346; E-mail: lorenzo.marrucci@na.infn.it

[1–4]. A nonzero photonic OAM appears in the "helical modes" of light, i.e., optical waves characterized by a helical-shaped wavefront and a single optical vortex at the beam axis. These waves have been shown to carry an OAM per photon directed as the beam axis z and equal to $L_z = m\hbar$, where m is an integer, in addition to the standard angular momentum associated with polarization, called *spin angular momentum* (SAM). Quantum information can be encoded in OAM by preparing photons in superpositions of different OAM modes. Being OAM an unlimited discrete variable, a single photon can carry many qubits at the same time, or alternatively a single so-called "*qudit*", i.e., a quantum state defined in a space having dimension $d > 2$. This makes the use of OAM very interesting for quantum information, at least in principle [4]. However, up to now the use of OAM has been hindered by its inconvenient and inefficient manipulation, leading to large photon losses and difficult implementations of quantum protocols. Moreover, a way to "interface" the OAM encoding with the commonly adopted polarization encoding has been missing so far.

A new tool for tackling these obstacles so as to open the way to a wider exploitation of the photon OAM in quantum information has been recently introduced by some of the authors of this paper [5–7]: the so-called "q-plate", a LC planar cell having certain specific singular-patterned orientation of the LC molecular director across the cell transverse plane. A q-plate introduces a coupling between the polarization and the OAM of light, allowing for the inter-conversion of these two forms of angular momentum [5,8]. In prospect, q-plates may find many photonic applications, ranging from particle manipulation in optical tweezers to OAM-based optical communication [6]. Promising for future integrated photonics applications, microscopic q-plates have been recently demonstrated in the form of liquid crystal droplets with radial alignment [9], exploiting an idea originally proposed by one of the authors of the present paper (L.M.) [10] and arising, in turn, from a former investigation of the light-induced manipulation of liquid crystal droplets [11]. However, the most interesting future applications of q-plates and related optical phenomena likely lie in the OAM-based quantum information field. In this paper we will review our recent results obtained in this direction, focusing mainly on the fundamental ideas and physical principles, while referring to the original works for most experimental details.

Photon Quantum States of Spin and Orbital Angular Momentum

A single photon having a well defined polarization and OAM state, that is occupying the corresponding optical mode, can be formally represented by a ket $|\psi\rangle = |\text{SAM}\rangle |\text{OAM}\rangle = |h\rangle_\pi |m\rangle_o$, where we are using the subscripts π and o to denote respectively the polarization and OAM spaces, and where the index h indicates one of two possible basis polarization states (i.e., either L, R or H, V) and the index m an integer (actually, to completely define the photon transverse mode we should add a third index specifying the radial profile, but hereafter we will omit it for brevity, as it plays no significant role [12]). However, in general a photon can also exist in an arbitrary superposition of these basis modes, i.e., $|\psi\rangle = \sum_{h,m} c_{h,m} |h\rangle_\pi |m\rangle_o$. For practical reasons, the infinite OAM space is actually always restricted to a finite-dimensional subspace. Very important are for example the bidimensional subspaces generated by opposite OAM values $\pm |m|\hbar$, which will be denoted as $o_{|m|}$. These subspaces can be conveniently used for encoding a single OAM qubit. For example, the state $|\psi\rangle = \alpha|+2\rangle_o + \beta|-2\rangle_o$ defines a qubit "written" in the OAM subspace o_2. These subspaces are important for two reasons: (i) the qubits are stable during free-space propagation, and (ii) they have a

full analogy with the standard polarization space. In the following we will only focus on the OAM subspace o_2 of photons, that is easily accessible with q-plates having $q = 1$, the only ones that we have used thus far.

The analogy with polarization also allows one to define an OAM Poincaré sphere to describe all possible OAM quantum states [13].

Quantum Effect of a q-Plate on a Single Photon

In this paper we will consider only q-plates with parameter $q = 1$, corresponding to a circularly symmetric pattern of the LC director around a center, such as a pure radial or azimuthal one. Moreover, we assume that the q-plates are "well tuned", that is their overall birefringent retardation is π (half-wave) for the working wavelength λ. This can be easily accomplished, for instance by thermal tuning [14].

The optical effect of a q-plate on a single photon is essentially the same as for a classical optical fields. For an input photon that is in a eigenstate of SAM, that is in a circular-polarized state, the spin-to-orbital conversion gives rise to the transformations shown in Figure 1. More interesting from the quantum information point of view is what happens with photons that are in a superposition of SAM eigenstates, that is in a arbitrary input polarization state. In this case, the q-plate is expected to act as a coherent device and hence preserve the superposition. Therefore, we should have the following transformation law:

$$|\psi\rangle = \alpha |L\rangle_\pi |0\rangle_o + \beta |R\rangle_\pi |0\rangle_o \xrightarrow{\text{q-plate}} \alpha |R\rangle_\pi |+2\rangle_o + \beta |L\rangle_\pi |-2\rangle_o \tag{1}$$

In the particular case of a linearly-polarized input, either H or V, we obtain the following [15]:

$$\begin{aligned}
|H\rangle_\pi |0\rangle_o &= \tfrac{1}{\sqrt{2}}\left(|L\rangle_\pi + |R\rangle_\pi\right)|0\rangle_o \xrightarrow{\text{q-plate}} \tfrac{1}{\sqrt{2}}\left(|R\rangle_\pi |+2\rangle_o + |L\rangle_\pi |-2\rangle_o\right) \\
|V\rangle_\pi |0\rangle_o &= \tfrac{1}{i\sqrt{2}}\left(|L\rangle_\pi - |R\rangle_\pi\right)|0\rangle_o \xrightarrow{\text{q-plate}} \tfrac{1}{i\sqrt{2}}\left(|R\rangle_\pi |+2\rangle_o - |L\rangle_\pi |-2\rangle_o\right)
\end{aligned} \tag{2}$$

The right-hand-side expressions can be interpreted as *entangled states* of the polarization and OAM degrees of freedom of the same photon (of course this kind of single-particle entanglement does not involve non-locality effects).

These predictions have been tested experimentally on single photon states obtained by parametric fluorescence [16]. In the output, the OAM analysis was

$$|L\rangle_\pi |0\rangle_o \Rightarrow \text{⊚} \Rightarrow |R\rangle_\pi |+2\rangle_o$$

$$|R\rangle_\pi |0\rangle_o \Rightarrow \text{⊚} \Rightarrow |L\rangle_\pi |-2\rangle_o$$

Figure 1. Effect of a q-plate (assumed to be well tuned and having $q = 1$) on a input photon that is in a circular-polarization and zero-OAM quantum state: the spin is inverted and the variation of SAM is entirely converted into OAM, that thus acquires $\pm 2\hbar$ of angular momentum (i.e., the output $m = \pm 2$).

Input *H* photons
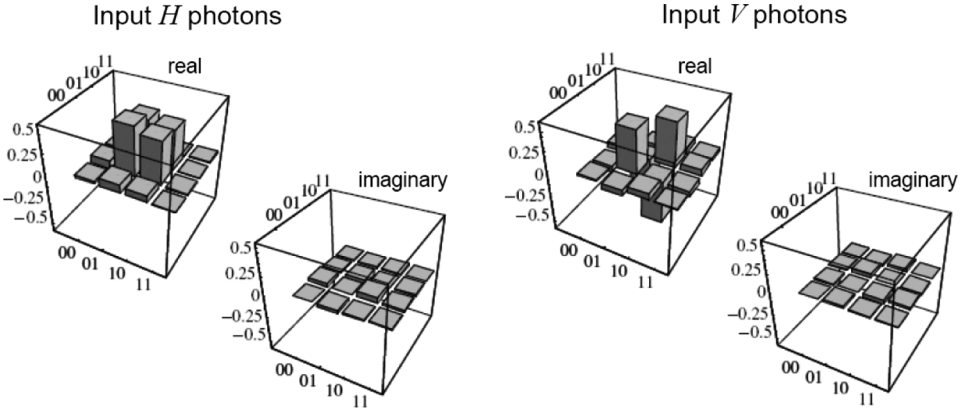
Input *V* photons

Figure 2. Results of experimental quantum tomography of the photons emerging from a q-plate for a linearly polarized input, either *H* or *V*. Represented are the measured real and imaginary parts of the photon density matrix (up to a common phase) [16]. The two degrees of freedom corresponding to the horizontal coordinates (the rows and columns of the density matrix) are polarization and OAM, taking the possible values *L*, *R* and +2, −2, respectively.

performed by using suitable fork-like holograms. An example of the experimental density matrices of photons having the polarization-OAM entangled states generated by a q-plate, as given by Eqs. (2), is shown in Figure 2. More details about the experimental setup used for these tests can be found in Ref. [16].

Quantum Information SAM ↔ OAM Transfer Devices

An interesting application of the q-plate is for realizing optical devices that can transfer the quantum information initially stored in the polarization degree of freedom of the photon into the OAM degree of freedom, or vice versa. In other words, these devices implement the following transformations:

$$
\begin{aligned}
\text{SAM} \to \text{OAM qubit transfer}: & \quad |\psi\rangle_\pi |0\rangle_o \longrightarrow |H\rangle_\pi |\psi\rangle_{o_2} \\
\text{OAM} \to \text{SAM qubit transfer}: & \quad |H\rangle_\pi |\psi\rangle_{o_2} \longrightarrow |\psi\rangle_\pi |0\rangle_o
\end{aligned} \tag{3}
$$

where the qubit state ψ here stands for any superposition of the basis states as defined by the coefficients α, β, and we are conventionally defining the linear polarization H as "reset" state, i.e., to be used when the polarization degree of freedom carries no information.

The simplest approach to realizing these transfer devices is illustrated in Figure 3: a combination of a q-plate and a polarizer for the SAM → OAM transfer and a combination of a q-plate and a coupler into a single-mode fiber (that selects only the $m = 0$ Gaussian mode) for the inverse OAM → SAM transfer. Their working principle is respectively based on the following transformations:

SAM → OAM:

$$
\begin{aligned}
|\psi\rangle_\pi |0\rangle_o = \left(\alpha|L\rangle_\pi + \beta|R\rangle_\pi\right)|0\rangle_o & \xrightarrow{\text{q-plate}} \alpha|R\rangle_\pi |+2\rangle_o + \beta|L\rangle_\pi |-2\rangle_o \\
& \xrightarrow{H\text{-polarizer}} \tfrac{1}{\sqrt{2}}|H\rangle_\pi \left(\alpha|+2\rangle_o + \beta|-2\rangle_o\right) = \tfrac{1}{\sqrt{2}}|H\rangle_\pi |\psi\rangle_o
\end{aligned} \tag{4}
$$
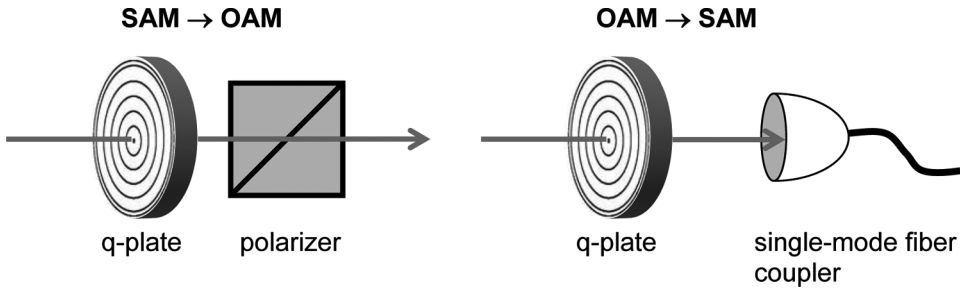
Figure 3. Pictorial representation of the simplest devices for the transfer of a qubit of quantum information from the polarization to the OAM (SAM → OAM) and vice versa (OAM → SAM).

OAM → SAM:

$$
\begin{aligned}
|H\rangle_\pi |\psi\rangle_o = |H\rangle_\pi \left(\alpha |+2\rangle_o + \beta |-2\rangle_o\right) &\xrightarrow{\text{q-plate}} \frac{\alpha}{\sqrt{2}}\left(|R\rangle_\pi |+4\rangle_o + |L\rangle_\pi |0\rangle_o\right) + \\
&+ \frac{\beta}{\sqrt{2}}\left(|R\rangle_\pi |0\rangle_o + |L\rangle_\pi |-4\rangle_o\right) \xrightarrow{\text{single-mode fiber coupling}} \frac{1}{\sqrt{2}}\left(\alpha |L\rangle_\pi + \beta |R\rangle_\pi\right)|0\rangle_o = \frac{1}{\sqrt{2}}|\psi\rangle_\pi |0\rangle_o
\end{aligned}
\tag{5}
$$

where the q-plate "*m*-shifting" action on input states having nonzero OAM has been used in the latter [5–7].

These transfer devices have been experimentally realized and tested [16,17], and typical transfer quantum fidelities of 98% were obtained. Even multiple transfers were successfully demonstrated, such as a forward-backward SAM → OAM → SAM, and the cascaded transfer SAM → OAM o_2 → OAM o_4, leading to writing a qubit in the OAM subspace with $m = \pm 4$ [17].

This implementation of the transfer devices is probabilistic, being successful only 50% of the times, due to the projection operations associated with the polarizer or the fiber-coupling. It is however also possible to obtain a fully deterministic transfer by adopting a suitable interferometer scheme, as discussed in Ref. [17].

Generating a Biphoton State with OAM Quantum Correlations

The single photon manipulations discussed above, although performed in the triggered mode ensuring the presence of one and only one photon at the time, are not truly different from classical optics experiments. Uniquely quantum effects that cannot be explained with classical theories only arise when dealing with more than one particle.

We have performed a first experiment aimed at generating a biphoton state with nontrivial OAM quantum correlations. A biphoton state is a single optical mode having exactly two photons. To this purpose, we started with a biphoton state having polarization correlations and than used the SAM → OAM transfer device to generate the final state.

The biphoton having polarization correlations has been obtained by collinear parametric fluorescence using type-II phase-matching, so as to have pairs of photons

that are orthogonally polarized. Such a state exhibits non-classical correlations if analyzed in circular-polarized states. To see it, let us consider the following state

$$|\psi\rangle = |H\rangle_1 |V\rangle_2 = \frac{1}{\sqrt{2}}(|L\rangle_1 + |R\rangle_1)\frac{1}{i\sqrt{2}}(|L\rangle_2 - |R\rangle_2) = \frac{1}{2i}(|L\rangle_1|L\rangle_2$$
$$+ |R\rangle_1|L\rangle_2 - |L\rangle_1|R\rangle_2 - |R\rangle_1|R\rangle_2) \tag{6}$$

where the two photons have been considered as distinguishable and therefore labelled 1 and 2. Experimentally, the photons are undistinguishable if they are well superimposed in space and time. They can be artificially made distinguishable for example by delaying them in time by inserting a birefringent crystal, thus exploiting their different polarization and the fact that the photons are generated in short pulses. If now we make the two photons become identical (except for the polarization), a two-particle quantum interference effect takes place, corresponding to the cancellation of the two intermediate terms in the right-hand-side of Eq. (6). The 2-photon state is thus transformed into the following (actually a correct formalism for calculating and representing this state for identical photons would require using the creation operators, but here we adopt a simplified notation to give the main idea):

$$|\psi\rangle = \frac{1}{i\sqrt{2}}(|L\rangle|L\rangle - |R\rangle|R\rangle) \tag{7}$$

This 2-photon state exhibits correlations in the circular-polarization states, as the two photons, despite each having a totally random polarization, always have the same polarization. After the SAM → OAM transfer device, the state above is converted into the following:

$$|\psi\rangle = \frac{1}{i\sqrt{2}}(|+2\rangle|+2\rangle - |-2\rangle|-2\rangle) \tag{8}$$

that is the desired biphoton state with OAM correlations. If the two photons are not identical, the quantum transfer preserves also the opposite-OAM terms, similar to Eq. (6). The successful generation of state (8) has been experimentally demonstrated by analyzing the output mode with a double-fork hologram, so as to separate photons carrying opposite OAM values in two opposite diffraction orders, and then detecting their coincidences, as shown in Figure 4. Since the two photons in state (8) have the same OAM, they will always be diffracted together and give rise to (ideally) zero coincidences. Delaying one of the photons so as to make them distinguishable will recover the terms in which the photons have opposite OAM and the coincidences will reappear. Figure 5

Photons "separator" (introducing a delay)
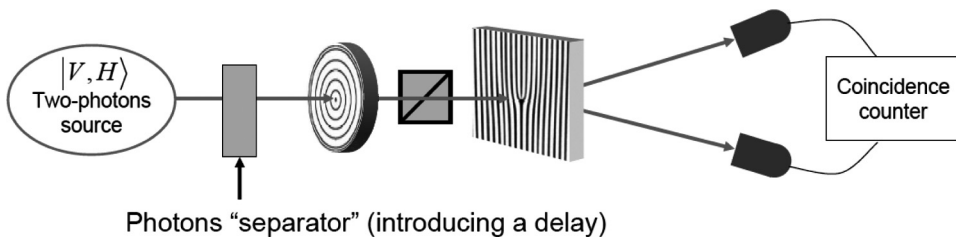
Figure 4. Sketch of the experimental scheme used for generating a biphoton state with OAM correlations and for testing it.
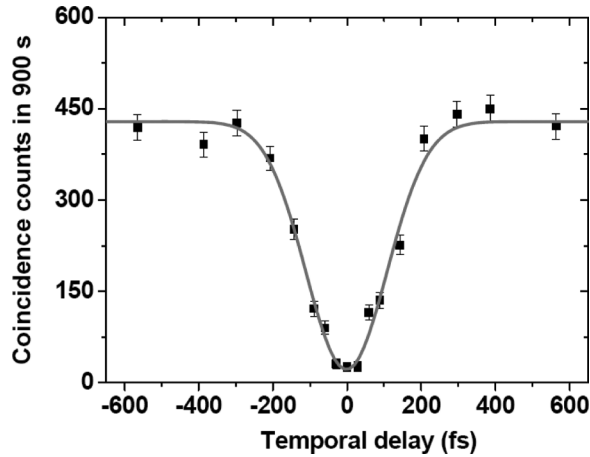
Figure 5. Coincidence counts obtained in the measurement of opposite OAM values for the biphoton generated by the q-plate, as illustrated in Figure 4 [16]. For zero delay the coincidence counts vanish (except for a small background), showing that the OAM of the two photons is fully correlated.

shows our experimental results [16], confirming the vanishing of the coincidences when the two photons precisely overlap. We have also performed other tests on this biphoton state, including a verification of the enhanced coalescence probability in OAM and a test of coherence based on analyzing the two photons in OAM-superposition states by suitable holograms. We refer the readers to Ref. [16] for further details.

Hong-Ou-Mandel Coalescence Effect with OAM-Carrying Photons

Thanks to the SAM $\rightarrow$ OAM and OAM $\rightarrow$ SAM quantum transfer devices, we can prepare an arbitrary qubit photon state in the SAM space and then transfer it to OAM and we can analyze any OAM state by simply transferring it back to the SAM space. This makes the OAM utilization in quantum photonic experiments much easier than it was before. As a first example of the versatility of this approach, we have performed the first experiment of Hong-Ou-Mandel (HOM) coalescence of OAM-carrying photons in a beam splitter (BS) [18].

The basic idea is illustrated in Figure 6, where two OAM-carrying photons are assumed to impinge on two input faces of a balanced BS (having 50% transmission and reflection probability). If the OAM states of these ingoing photons are opposite, a two-particle quantum interference takes place and the two photons will emerge always together from the same output port of the BS. If the ingoing photons have the same OAM, the interference is destroyed because the emerging photons can be distinguished by their OAM state.

The quantum coalescence can be detected by looking at the vanishing coincidences on the two output sides of the BS, or by looking only at one output port and observing a doubled number of photon pairs. For practical reasons we have adopted the latter method. The results of our measurements are shown in Figure 7: the coalescence effect is clearly demonstrated as well as its switching on and off by varying the input OAM state of photons [18]. The importance of this proof-of-principle demonstration is that the HOM coalescence effect is an enabling process, on which many quantum
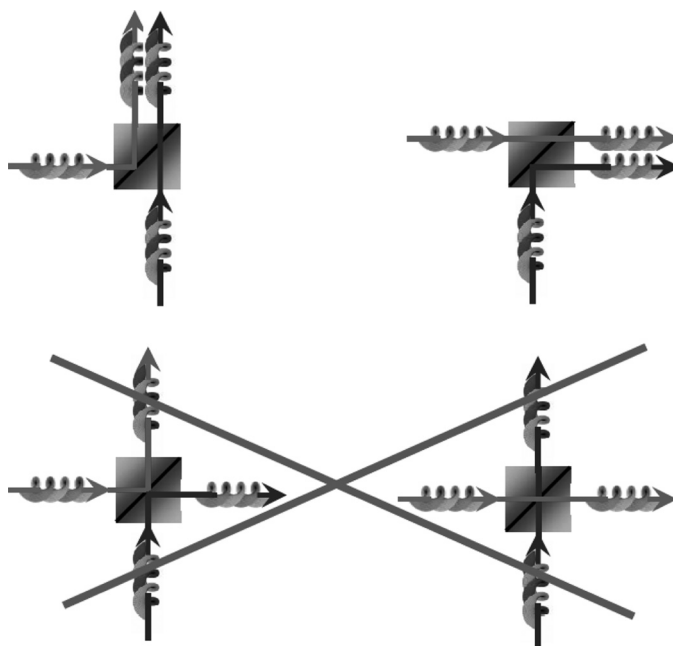
Figure 6. Pictorial illustration of the Hong-Ou-Mandel two-photon interference effect in a beam-splitter for the case of OAM-carrying photons (depicted as little helices). In this example the input OAM of the two photons is opposite, so that if one of the two photon is reflects it is inverted and becomes equal to that of the other photon. It can then be shown that the two processes in the lower panels, leading to exactly the same final state, have opposite amplitudes and cancel (as long as the two photons are otherwise identical). The remaining two processes in the upper panel have a doubled probability of taking place, so that one obtains an enhanced quantum coalescence of the photons in the output ports of the beam-splitter. If the input OAM of the two photon is equal, the interference does not take place because all processes give rise to different outputs and there is no enhancement.

information protocols are based (such as the quantum teleportation, quantum cloning, etc.). In the next section, we start putting it to work by demonstrating the quantum cloning of qubits encoded in the OAM degree of freedom of single photons.

Optimal Quantum Cloning of OAM-Carrying Photons

An unknown qubit ψ cannot be copied without error. This is a consequence of the principles of quantum mechanics, as proved in the so-called *quantum no-cloning theorem*. It is however still possible to make an imperfect copy, with a maximum quantum fidelity $F = 5/6$. This corresponds to saying that the copied qubit has a $5/6$ probability of being exactly equal to the qubit to be copied and a $1/6$ probability of being orthogonal to it. The copied qubit is in mixed state that can be described by the following density matrix:

$$\hat{\rho}_{\text{cloned}} = \frac{5}{6}|\psi\rangle\langle\psi| + \frac{1}{6}|\psi^{\perp}\rangle\langle\psi^{\perp}| \tag{9}$$

where $\psi^{\perp}$ stands for the state orthogonal to ψ.
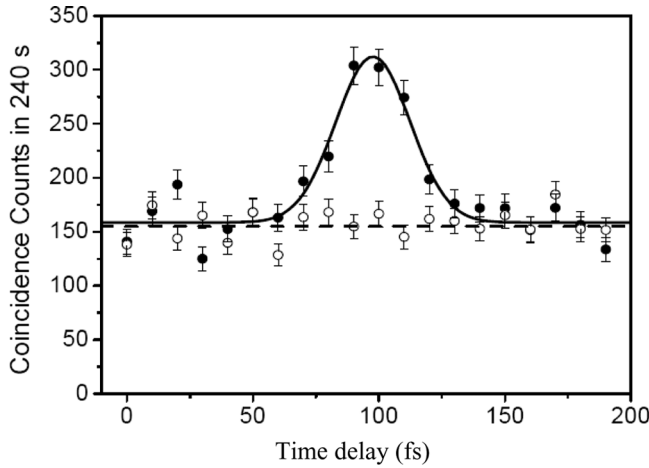
Figure 7. Concidence counts detected for the OAM-carrying photons emerging from a beam splitter in a HOM experiments, after separating the two photons by a second beam-splitter [18]. Full circles refer to opposite input OAM states, showing the enhanced coalescence for the delay giving the correct overlap of the two photons, and open circles refer to equal input OAM states, giving no coalescence enhancement.

There exist different demonstrated approaches to implementing the optimal quantum cloning of photons. A particularly simple one is that based on the so-called symmetrization technique, involving the HOM coalescence effect in a BS [19]. This technique has been already demonstrated with polarization [19], and now it becomes possible to replicate such results with OAM photon qubits. The working principle, illustrated in Figure 8, is based on the introduction of the photon to be cloned, carrying a OAM qubit $|\psi\rangle = \alpha|+2\rangle + \beta|-2\rangle$, in one of the two input ports of the BS, and of an ancilla photon in a totally random mixed state $\hat{\rho} = \frac{1}{2}(|+2\rangle\langle+2| + |-2\rangle\langle-2|)$ in the other input port. The output is given by the two photons that are emerging from the
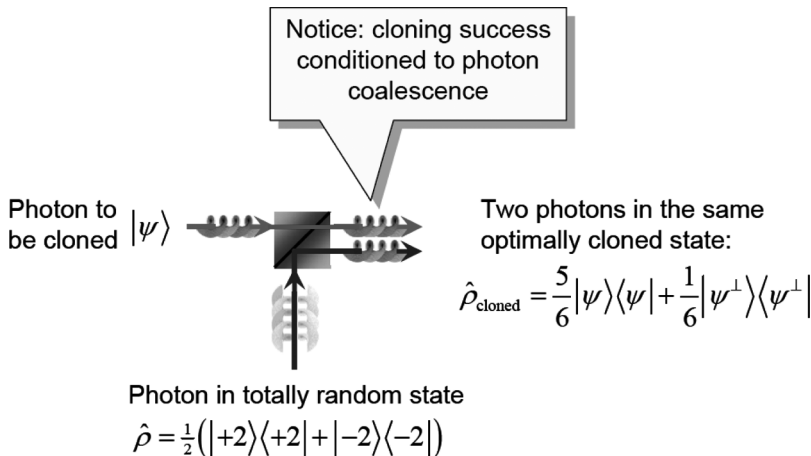
Figure 8. Pictorial illustration of the optimal quantum cloning based on the symmetrization method in a beam-splitter for the case of OAM-qubit-carrying photons.
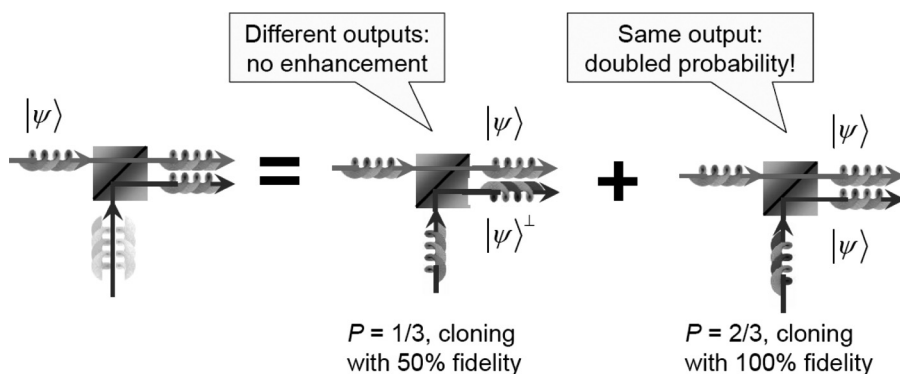
Figure 9. Graphical analysis of the cloning quantum fidelity.

same output port of the BS. The cloning will be successful only when the two photons came out together from such a port, otherwise the process fails. Therefore this implementation is a probabilistic one, and it can be shown that its success probability is 3/8 (if using only one output port of the BS, it is doubled to 3/4 if both ports are used). Now, the randomized photon, after being reflected in the BS, can be considered as a mixture of a photon having state $|\psi\rangle$ and state $|\psi^\perp\rangle$, with equal probabilities. Since the probability of the two photons of coming out together is doubled when the output photons are in the same state, it is easy to see that the output will correspond to two identical photons for 2/3 of the times and to two orthogonal photons for 1/3 of the times. Each photon of the output pair will therefore have $2/3 \times 100\% + 1/3 \times 50\% = 5/6$ probability of being identical to the input photon to be copied and this is just the optimal fidelity. This simple argument is illustrated in Figure 9.

We have experimentally demonstrated this optimal cloning by preparing the two input photons by means of the q-plate SAM → OAM quantum transfer devices and by analyzing the output after a OAM → SAM transfer [18]. The randomized photon was obtained by randomizing the polarization before the transfer (by a random rotation of waveplates). The cloned photons were found to have an average fidelity of about 0.80 to the input one, fully compatible with the 5/6 expectation value after taking into account the finite fidelity of the quantum transfer devices.

Conclusions

In this brief review we have illustrated the recent progresses that have been made in controlling the orbital angular momentum degree of freedom of photons in the quantum domain, thanks to a simple optical element based on patterned liquid crystals. This progress is already opening the way to a wider exploitation of orbital angular momentum in quantum information tasks with photons (see, e.g., Ref. [20]). Ideally, manipulating the orbital angular momentum of light in the classical as well as in the quantum domain is becoming almost as simple as for polarization, thanks to liquid crystal devices.

References

[1] Franke-Arnold, S., Allen, L., & Padgett, M. J. (2008). *Laser & Photon. Rev.*, *2*, 299.
[2] Mair, A., Vaziri, A., Weihs, G., & Zeilinger, A. (2001). *Nature*, *412*, 313.

[3] O'Neil, A. T., MacVicar, I., Allen, L., & Padgett, M. J. (2002). *Phys. Rev. Lett.*, *88*, 053601.

[4] Molina-Terriza, G., Torres, J. P., & Torner, L. (2007). *Nature Phys.*, *3*, 305.

[5] Marrucci, L., Manzo, C., & Paparo, D. (2006). *Phys. Rev. Lett.*, *96*, 163905.

[6] Marrucci, L., Manzo, C., & Paparo, D. (2006). *Appl. Phys. Lett.*, *88*, 221102.

[7] Marrucci, L. (2008). *Mol. Cryst. Liq. Cryst.*, *488*, 148.

[8] Karimi, E., Piccirillo, B., Marrucci, L., & Santamato, E. (2009). *Opt. Lett.*, *34*, 1225.

[9] Brasselet, E., Murazawa, N., Misawa, H., & Juodkazis, S. (2009). *Phys. Rev. Lett.*, *103*, 103903.

[10] Marrucci, L. *12th Int. Topical Meeting on Optics of Liquid Crystals* (OLC07), filed as e-LC preprint at http://www.e-lc.org/presentations/docs/2008_01_16_12_47_07/.

[11] Manzo, C., Paparo, D., Marrucci, L., & Jánossy, I. (2006). *Phys. Rev. E*, *73*, 051707.

[12] Karimi, E., Zito, G., Piccirillo, B., Marrucci, L., & Santamato, E. (2007). *Opt. Lett.*, *32*, 3053.

[13] Padgett, M. J., & Courtial, J. (1999). *Opt. Lett.*, *24*, 430.

[14] Karimi, E., Piccirillo, B., Nagali, E., Marrucci, L., & Santamato, E. (2009). *Appl. Phys. Lett.*, *94*, 231124.

[15] Marrucci, L. (2007). *Proceedings of SPIE*, *6587*, 658708.

[16] Nagali, E., Sciarrino, F., De Martini, F., Marrucci, L., Piccirillo, B., Karimi, E., & Santamato, E. (2009). *Phys. Rev. Lett.*, *103*, 013601.

[17] Nagali, E., Sciarrino, F., De Martini, F., Piccirillo, B., Karimi, E., Marrucci, L., & Santamato, E. (2009). *Opt. Express*, *17*, 18745.

[18] Nagali, E., Sansoni, L., Sciarrino, F., De Martini, F., Marrucci, L., Piccirillo, B., Karimi, E., & Santamato, E. (2009). *Nature Photonics*, *3*, 720.

[19] Ricci, M., Sciarrino, F., Sias, C., & De Martini, F. (2004). *Phys. Rev. Lett.*, *92*, 047901.

[20] Chen, L. X., & She, W. L. (2009). *New J. Phys.*, *11*, 103002.